

# Design of Linear mmWave Wideband Mixer-first Receivers

*Rawan Al Kubaisy*  
*Ali Niknejad, Ed.*



Electrical Engineering and Computer Sciences  
University of California, Berkeley

Technical Report No. UCB/EECS-2025-16

<http://www2.eecs.berkeley.edu/Pubs/TechRpts/2025/EECS-2025-16.html>

May 1, 2025

Copyright © 2025, by the author(s).  
All rights reserved.

Permission to make digital or hard copies of all or part of this work for personal or classroom use is granted without fee provided that copies are not made or distributed for profit or commercial advantage and that copies bear this notice and the full citation on the first page. To copy otherwise, to republish, to post on servers or to redistribute to lists, requires prior specific permission.

---

# Design of Linear mmWave Wideband Mixer-first Receivers

by Rawan Al Kubaisy

---

## Research Project

Submitted to the Department of Electrical Engineering and Computer Sciences,  
University of California at Berkeley, in partial satisfaction of the requirements for the  
degree of **Master of Science, Plan II**.

Approval for the Report and Comprehensive Examination:

### Committee:



---

Professor Ali Niknejad  
Research Advisor

12/12/2022

---

(Date)

\* \* \* \* \*



---

Professor Vladimir Marko Stojanovic  
Second Reader

1/9/2023

---

(Date)

Design of Linear mmWave Wideband Mixer-first Receivers

by

Rawan Al Kubaisy

A thesis submitted in partial satisfaction of the  
requirements for the degree of

Master of Science

in

Electrical Engineering and Computer Sciences

in the

Graduate Division

of the

University of California, Berkeley

Committee in charge:

Professor Ali M. Niknejad, Chair  
Professor Vladimir Marko Stojanovic

Fall 2022

Design of Linear mmWave Wideband Mixer-first Receivers

Copyright 2022

by

Rawan Al Kubaisy

## Abstract

Design of Linear mmWave Wideband Mixer-first Receivers

by

Rawan Al Kubaisy

Master of Science in Electrical Engineering and Computer Sciences

University of California, Berkeley

Professor Ali M. Niknejad, Chair

A 25-40GHz passive mixer-first receiver using a novel architecture for digital beamforming arrays is proposed. The architecture uses a novel technique for impedance matching using the on-resistance of the mixers in the receiver and matching networks. The small switch resistance of the mixers is matched to the antenna using matching networks. Several matching networks are discussed, including a tunable matching network for wideband applications. The design achieves a noise figure that is lower than 8dB, a conversion gain of 18dB, and an IIP3 of around +4dBm across the frequency range of 25-40GHz. A prototype chip is fabricated in 28nm bulk CMOS process.

# Contents

<b>Contents</b>	<b>i</b>
<b>List of Figures</b>	<b>ii</b>
<b>List of Tables</b>	<b>iv</b>
<b>1 Introduction</b>	<b>1</b>
<b>2 Wilkinson Divider in Mixer-first Receivers</b>	<b>5</b>
2.1 Wilkinson Divider . . . . .	5
2.2 Wilkinson Divider in Mixer-first Receivers . . . . .	7
2.3 Mixer-First Receiver with Modified Wilkinson Divider . . . . .	11
<b>3 Mixer-first Receiver with Tunable Matching Network</b>	<b>14</b>
3.1 Linearity . . . . .	16
3.2 Noise Figure . . . . .	20
3.3 Circuit Implementation . . . . .	21
3.4 Measurements . . . . .	27
<b>4 Conclusion and Future Work</b>	<b>28</b>
<b>Bibliography</b>	<b>31</b>
<b>A Isolation in Wilkinson Dividers</b>	<b>33</b>

# List of Figures

1.1	(a) Conventional 4-phase passive mixer-first receiver and non-overlapping LO waveforms. (b) Its LTI equivalent. . . . .	2
1.2	High linearity mixer-first receiver (a) full schematic and the overlapping LO waveforms. (b) The LTI equivalent. . . . .	4
2.1	Wilkinson divider. . . . .	5
2.2	Input matching with a Wilkinson divider (WD). The dashed line in (a) and (b) are the lines of symmetry (LOS). (a) Wilkinson Divider. (b) WD w/ open LOS (c) $\lambda/4$ transmission line transformation. (d) Total input impedance. . . . .	6
2.3	Mixer-first receiver with Wilkinson divider . . . . .	8
2.4	Noise figure of a receiver with a $50\Omega$ resistor and a receiver with a Wilkinson Divider designed for 20GHz with $R_{sw} = 12\Omega$ . . . . .	9
2.5	Mixer-first receiver with modified Wilkinson divider . . . . .	10
2.6	Noise figure of a receiver with a $50\Omega$ resistor, receivers with a $\lambda/4$ transmission lines designed for 20GHz . . . . .	11
2.7	Noise figure of receiver with a $50\Omega$ resistor and receiver with a $\lambda/4$ transmission line designed for 30GHz . . . . .	12
3.1	Mixer-first receiver with L-matching network . . . . .	15
3.2	Comparison of NF across three different RX designs. . . . .	16
3.3	Mixer-first receiver with tunable L-matching network. . . . .	17
3.4	Simplified schematics of figure 3.3 . . . . .	19
3.5	LTI equivalent circuits for figures 3.3 and 3.4. $R_{sh}$ is the re-radiation resistance and $R_{OL}$ is the overlap resistance. The two 8:1 matching networks in figure 3.4 can be replaced by one 4:1 matching network in the LTI model . . . . .	19
3.6	Noise figure values of the proposed linear receiver compared to the design proposed in the previous chapter. Ideal LO, baseband amplifier, and $R_{sw} = 6\Omega$ . . .	22
3.7	Inverter-based baseband amplifier . . . . .	22
3.8	Schematic of the LO Chain [6]. . . . .	23
3.9	Noise figure of Rx with fully tunable lossy L-matching networks, transistor switches, and LO chain . . . . .	24
3.10	Inductors' Layout . . . . .	25
3.11	Inductors Q and L . . . . .	25

3.12	Post-layout Simulations of the design . . . . .	26
3.13	Noise summary results . . . . .	26
3.14	Chip micrograph in 28 nm bulk CMOS process . . . . .	27
A.1	Differential and common mode schematics. (a) Wilkinson divider. (b) Wilkinson divider in common mode. (c) Wilkinson divider common mode half circuit. (d) Wilkinson divider in differential mode. (e) Wilkinson divider differential mode half circuit. . . . .	34

# List of Tables

4.1	Comparison with mixer-first receivers greater than 25GHz . . . . .	29
4.2	Comparison with recently published 28GHz receiver front-ends . . . . .	30

# Chapter 1

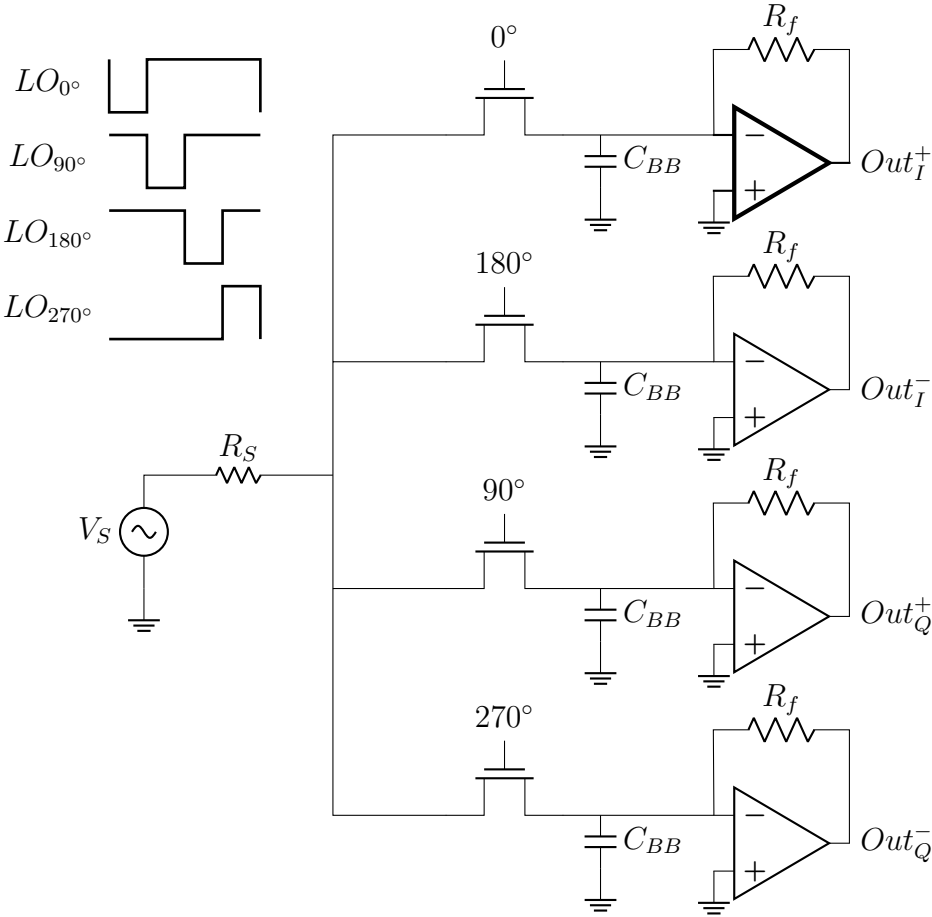
## Introduction

Digital beamforming arrays are an enabler to the 5G revolution. The increased number of users necessitates switching to higher frequencies with a large number of frequency bands, this includes the 24-40GHz band. The increasing number of bands in the mmWave spectrum mandates advanced circuit techniques to deal with the challenges associated with the high frequency and the large number of users. These challenges include linearity, interference mitigation, bandwidth, and other concerns. The use of digital beamforming arrays makes the linearity requirement more stringent but relaxes the noise figure requirement. This makes mixer-first receiver an attractive candidate for digital beamforming arrays because of their high linearity and their moderate noise figure.

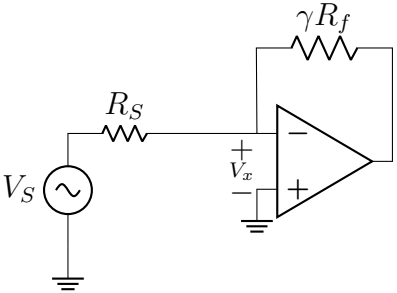
Figure 1.1 shows a conventional 4-phase passive mixer-first receiver driven by non-overlapping LO waveform. Traditionally, matching is done using the transparency property of N-path filters. Instead of using a shunt resistor, which will add a 3dB penalty to the noise figure, matching is done using miller's effect with the feedback resistor of the baseband amplifier. Using miller's effect, the impedance looking into the receiver from the antenna is equal to:

$$Z_{in} = \frac{\gamma R_f}{(1 + A(s))} \quad (1.1)$$

A high linearity mixer-first receiver for digital mmWave beamforming arrays was proposed in [7]. Figure 1.2.a shows the schematic of the highly linear receiver. The work achieves in-band IIP3 that are 16dB higher than the state-of-the-art passive mixer-first receivers. In [7], instead of using miller's effect of the feedback resistor of the baseband amplifier for



(a)



$V_x \approx 0$  by design  
 $\gamma = 2/\pi^2$

(b)

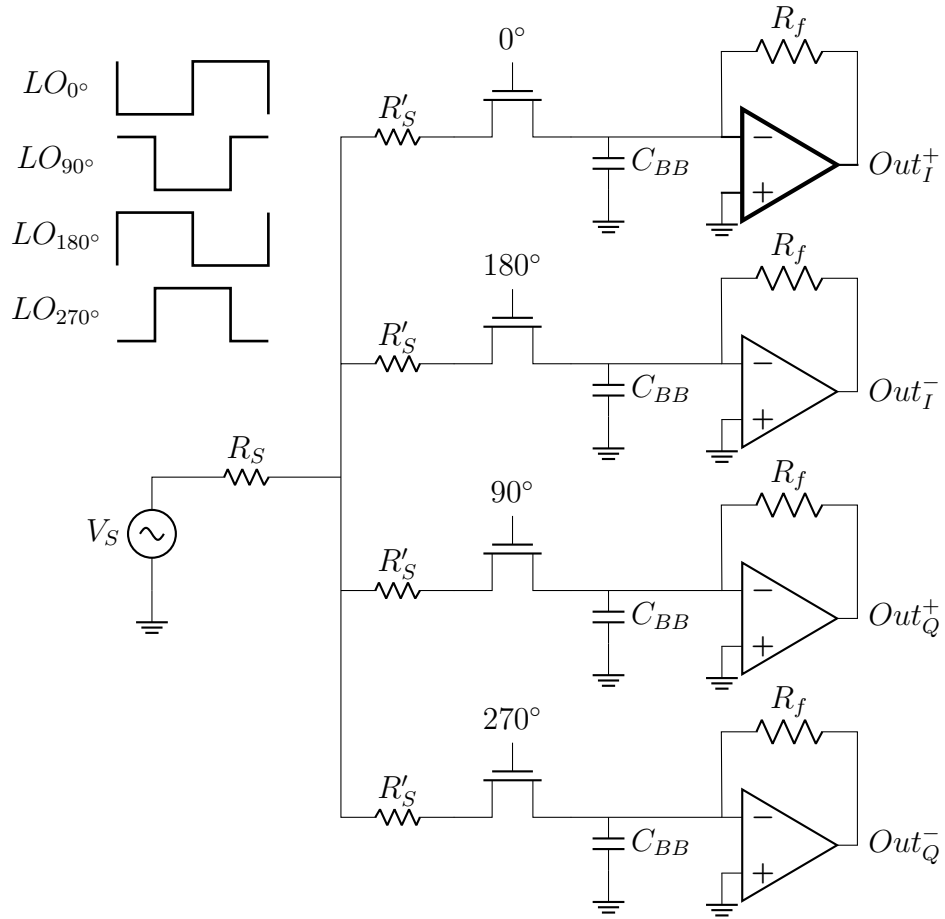
Figure 1.1: (a) Conventional 4-phase passive mixer-first receiver and non-overlapping LO waveforms. (b) Its LTI equivalent.

matching, matching is done with a  $50\Omega$  physical resistor. Additionally, the design uses feedback linearization to improve the linearity of the receiver.

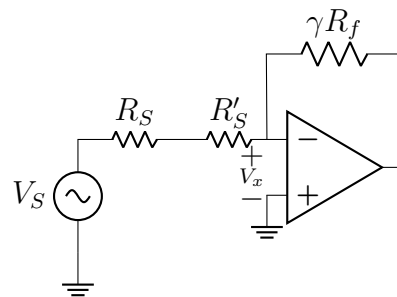
Feedback linearization is achieved by designing a baseband amplifier with a large open loop gain, making the voltage at the input of the baseband amplifier a virtual ground. The large loop gain of the baseband amplifier would make the impedance looking into the baseband amplifier small, reducing the swing at the input of the amplifier. The small input swing would translate to less distortion caused by the baseband amplifier. Figure 1.2.b shows an illustration of that where  $V_x$  is chosen to be approximately zero by design.

The noise figure of the design ranges from 12.5dB to 15.7dB for  $f_{RF}$  that ranges from 10GHz to 30GHz. The noise figure is high due to several factors. The use of the  $50\Omega$  resistors adds a 3.1dB penalty to the noise figure. Additionally, charge sharing plays a large role in degrading the noise figure of receivers with overlapping LO waveform. Synthesizing 25% duty-cycle LO Waveform at microwave and mmWave frequencies is challenging. Hence, a 50% duty-cycle LO is used in this design. The overlapping LO waveform results in charge sharing between the I and Q paths which will degrade the noise figure. The authors in [7] proposed using  $50\Omega$  resistors in all of the mixers' paths, instead of one  $50\Omega$  resistor to reduce the charge sharing. Although the addition of the resistors on all of the paths helped reduce charge sharing, the resistors would only reduce charge sharing current and not filter it out. On the other hand, the addition of resistors on all paths increased the parasitic capacitance leading to more loss in the signal path, and a further degradation in the noise figure.

In this thesis, we propose a linear receiver design to overcome noise figure limitation present in the high linearity receiver design proposed in [7]. The thesis proposes eliminating the use of the  $50\Omega$  resistors and using  $R_{on}$  of the mixers in addition to matching networks to achieve matching. This thesis is organized as follows. Chapter 2 explores a narrowband mixer-first receiver design using Wilkinson dividers and a modified version of the Wilkinson divider. Chapter 3 explores the use of L-matching networks in the receiver including a tunable matching network for wideband applications. Chapter 3 also discusses the circuit implementation of the wideband receiver and the post-layout simulations. Chapter 4 compares this work against other mixer-first receivers and provides the takeaway and possible ways to improve the design.



(a)



$V_x \approx 0$  by design  
 $\gamma = 2/\pi^2$

(b)

Figure 1.2: High linearity mixer-first receiver (a) full schematic and the overlapping LO waveforms. (b) The LTI equivalent.

# Chapter 2

## Wilkinson Divider in Mixer-first Receivers

This chapter explores the use of Wilkinson Dividers in mixer-first receivers. Two designs are analyzed, simulated, and compared to the linear receiver described in the previous chapter and in [7].

### 2.1 Wilkinson Divider

Figure 2.1 shows the schematic of a Wilkinson divider. Wilkinson dividers are used as either power combiners or power dividers. They have the benefit of isolating  $Port_2$  and  $Port_3$  while

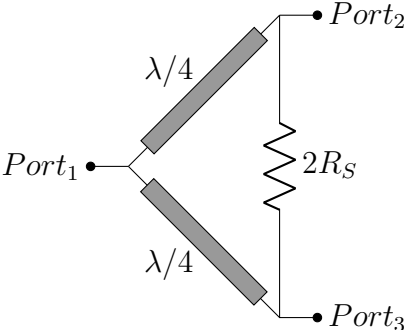


Figure 2.1: Wilkinson divider.

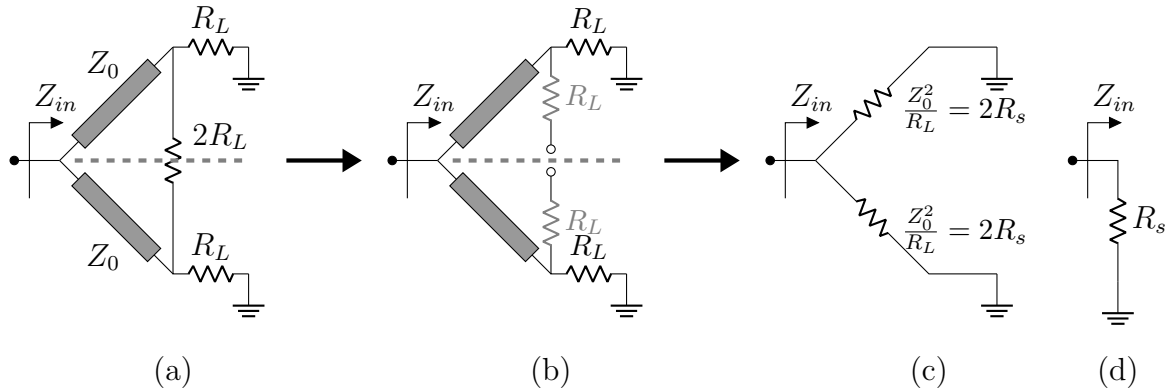


Figure 2.2: Input matching with a Wilkinson divider (WD). The dashed line in (a) and (b) are the lines of symmetry (LOS). (a) Wilkinson Divider. (b) WD w/ open LOS (c)  $\Lambda/4$  transmission line transformation. (d) Total input impedance.

providing impedance matching between  $Port_1$  and the other two ports. The two quarter-wavelength transmission lines provide input matching and help with the isolation between  $Port_2$  and  $Port_3$ .

Traditionally, the characteristic impedance of the transmission line is chosen to be  $50\Omega$  with  $50\Omega$  termination resistors at all ports. But since a quarter-wavelength transmission line can be used as an impedance transformer, the lines' characteristic impedance can be changed to achieve matching with load resistors that are not equal to  $50\Omega$ . Figure 2.2 shows how the input matching is achieved using common mode analysis.

When used as a power divider,  $Port_2$  and  $Port_3$ , which are the output ports, are isolated by current cancellation. This can be shown by calculating  $S_{23}$ .  $S_{23}$  can be calculated by applying a signal at  $Port_2$  and using differential and common mode circuit equivalent to calculate the total current flowing through the load resistor at  $Port_3$ . The current through the bridge resistor will be 180 degrees out of phase with the current through the transmission lines. This means that no current will flow through the load resistor at  $Port_3$ . In order for the two output ports to be isolated, the bridge resistor value has to be equal to  $2R_{sw}$ . This is discussed with further details in Appendix A.

## 2.2 Wilkinson Divider in Mixer-first Receivers

In the design proposed in [7], matching was achieved using a  $50\Omega$  physical resistor which added a 3.1dB penalty to the noise figure. In an effort to improve the noise figure of the receiver, this design proposes eliminating the  $50\Omega$  physical resistor and using a Wilkinson divider between the antenna and the mixers. Figure 2.3 shows the schematic of the design. Instead of a  $50\Omega$  resistor, the on-resistance of the mixers can be used for matching. And with the help of the quarter-wavelength transmission line, a small on-resistance of the mixers' can be transformed to a larger value to match the antenna. In theory, the addition of a Wilkinson divider will provide isolation between the I and the Q paths of the receiver, which are  $Port_2$  and  $Port_3$  of the Wilkinson Divider. This means that that the charge sharing current that is caused by the overlapping LO waveform will be reduced. This design uses feedback linearization proposed in [7] and discussed in chapter 1 to mitigate the effect of the baseband distortion on receiver's overall linearity. Feedback linearization means choosing a large open loop gain for the baseband amplifier which would result in a smaller voltage swing at the input of the baseband amplifier.

### Input Matching

The impedance matching can be achieved by choosing the width of the transmission line such that its characteristic impedance is

$$Z_0 = \sqrt{2R_{sw}R_S} \quad (2.1)$$

With the assumption that the negative terminal of the baseband amplifier is a virtual ground which makes  $Z_{in} = 0$ , the impedance looking into one transmission line equal to

$$Z_{Tline1} = \frac{Z_0^2}{R_{sw}} = \frac{2R_{sw}R_S}{R_{sw}} = 2R_S \quad (2.2)$$

And the input impedance looking into the receiver is

$$Z_{in} = 2R_S || 2R_S = R_S \quad (2.3)$$

Figure 2.4 shows the difference between the simulated noise figure of proposed receiver compared to the design with  $50\Omega$  physical resistors. The design is simulated using lossy

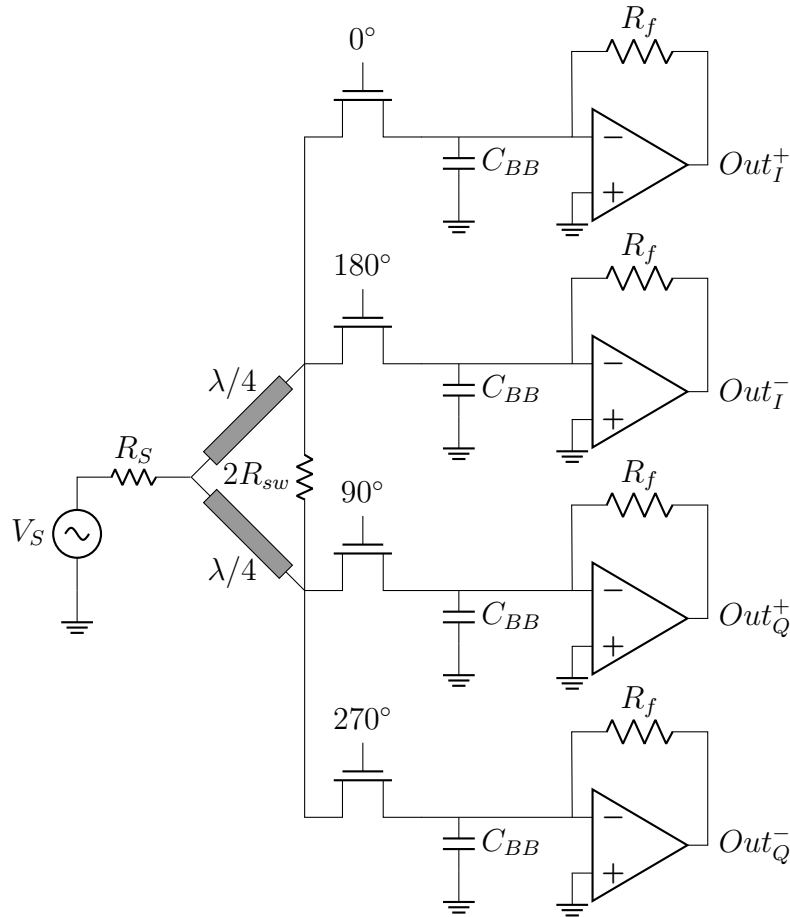


Figure 2.3: Mixer-first receiver with Wilkinson divider

transmission lines from rfTlineLib library. The width of the line is found using an online calculator to achieve matching to  $R_{SW} = 12\Omega$ . The transmission line length is 1.8 mm which is equal to equal to quarter wavelength at 20GHz. The baseband amplifier is an ideal differential amplifier with an open loop gain of 60dB, input capacitors of 500fF at the input of the baseband amplifier, and a feedback resistor of 1 k $\Omega$ . Ideal switches are used for the switches with an on-resistance of 12 $\Omega$ . The simulation results showed a 2.4dB improvement at 20GHz. The noise figure gets worse as the frequency shifts from 20GHz. This is expected since the input matching would not be achieved at other frequencies.

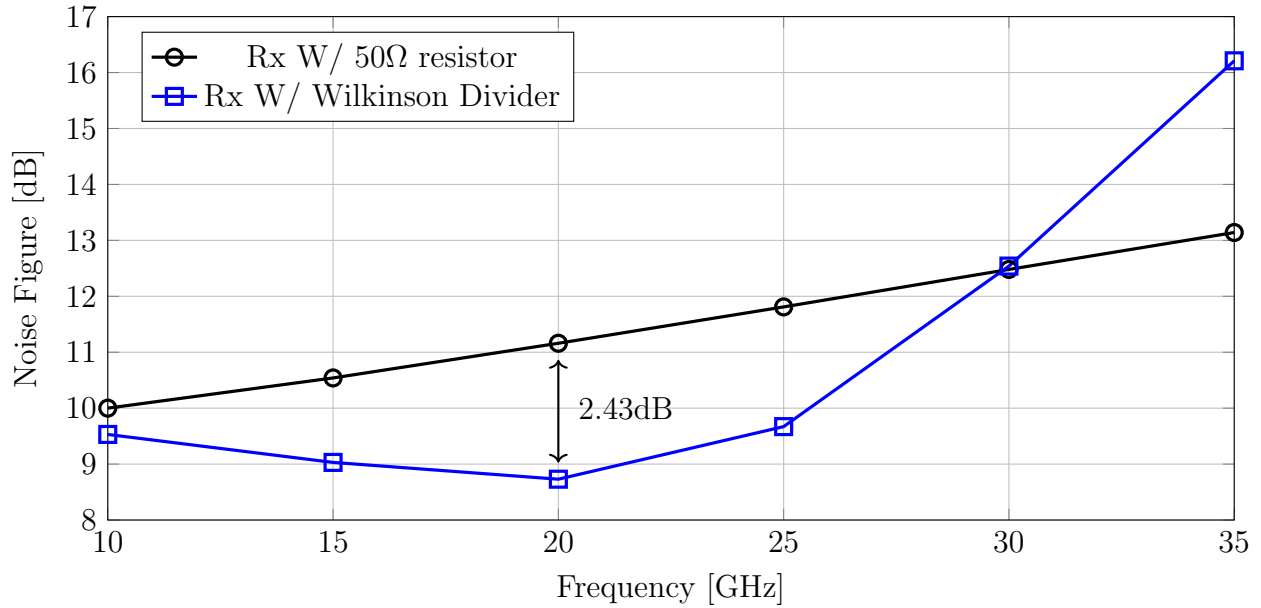


Figure 2.4: Noise figure of a receiver with a  $50\Omega$  resistor and a receiver with a Wilkinson Divider designed for 20GHz with  $R_{sw} = 12\Omega$

## Limitations

Although the new design employing the use of a wilkinson divider shows improvement in the noise figure. the use of a Wilkinson Divider in a mixer-first receiver has several drawbacks. Using a Wilkinson Divider makes the design narrowband. The matching between the input and the outputs only valid for a single frequency, which is the frequency where the length of the transmission line is a quarter wavelength. Wideband designs of Wilkinson divider employing the use of tapered transmission lines can be used. But the use of a wideband Wilkinson divider will increase the charge sharing current and will degrade the noise figure of the receiver.

The narrow-banded nature of the Wilkinson divider is not only related to the input matching, it's also related to the isolation between the two output ports,  $Port_2$  and  $Port_3$ . The two ports are only completely isolated if the signal applied at either  $Port_2$  or  $Port_3$  is at the same frequency that would result in a quarter wavelength equal to the transmission lines' lengths. Since the use of the Wilkinson divider in this design is to prevent the charge sharing current from getting to the adjacent path, it would not be as effective. The charge sharing

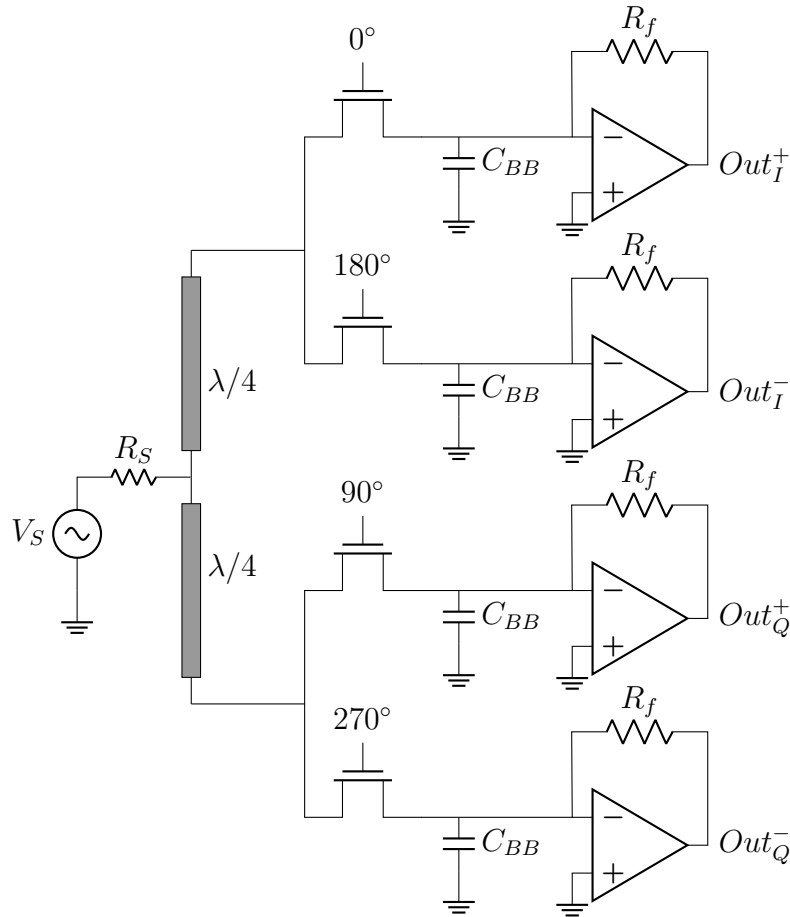


Figure 2.5: Mixer-first receiver with modified Wilkinson divider

current is the result of one capacitor at the input of baseband amplifier discharging and charging up the capacitor at the other baseband input. This means that the current sharing current is not a single tone and will not be fully suppressed by the Wilkinson Divider. The bridge resistor is providing more of a leakage path for the charge sharing current. Additionally, the noise of the bridge resistor is also adding to the noise of the receiver.

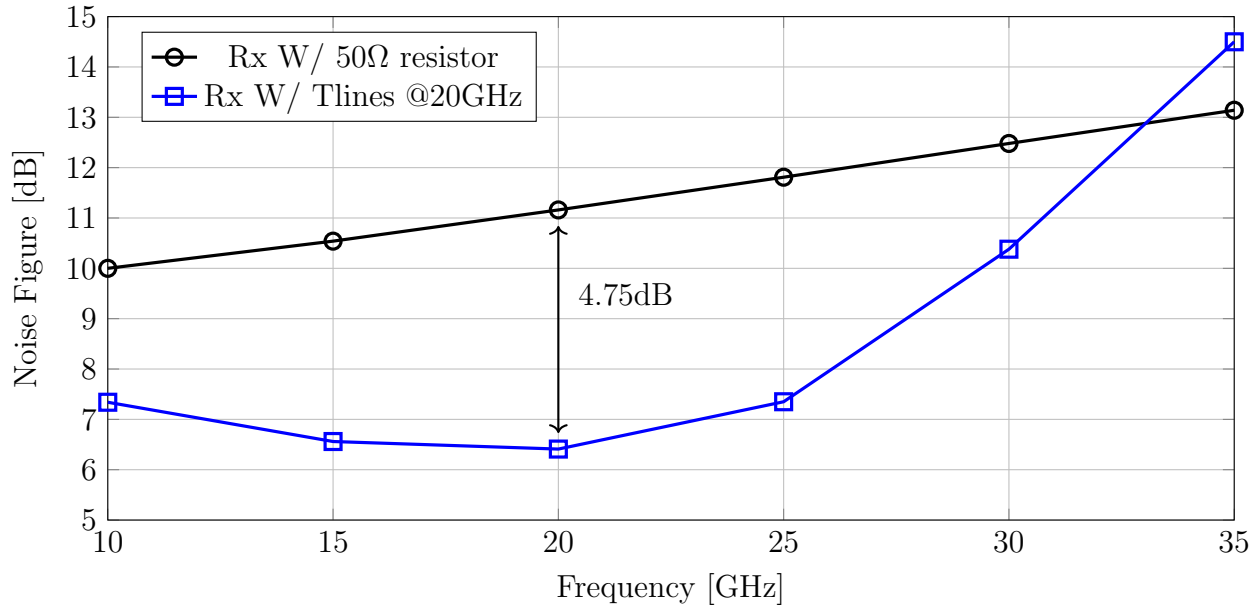


Figure 2.6: Noise figure of a receiver with a  $50\Omega$  resistor, receivers with a  $\lambda/4$  transmission lines designed for 20GHz

## 2.3 Mixer-First Receiver with Modified Wilkinson Divider

The second proposed design uses a modified version of a Wilkinson divider between the antenna and the mixers. common mode half circuit analysis in figure 2.2 shows that the bridge resistor does not contribute to the input matching because the bridge resistor is open in common mode. The main purpose of the resistor is to provide isolation between the  $Port_2$  and  $Port_3$ . The discussion at the end of section 2.2 showed that the bridge resistor doesn't help with suppressing the charge sharing current, and it might be increasing the charge sharing between the I and the Q paths and impacting the noise figure. Hence, the bridge resistor can be omitted from the design. The rest of the design is not changed from the previous architecture. The quarter-wavelength transmission lines are still used to transform the on-resistance of mixers to match the resistance of the antenna. Similar to the previous architecture, this design uses feedback linearization proposed in the previous section to mitigate the effect of the baseband distortion on receiver's overall linearity.

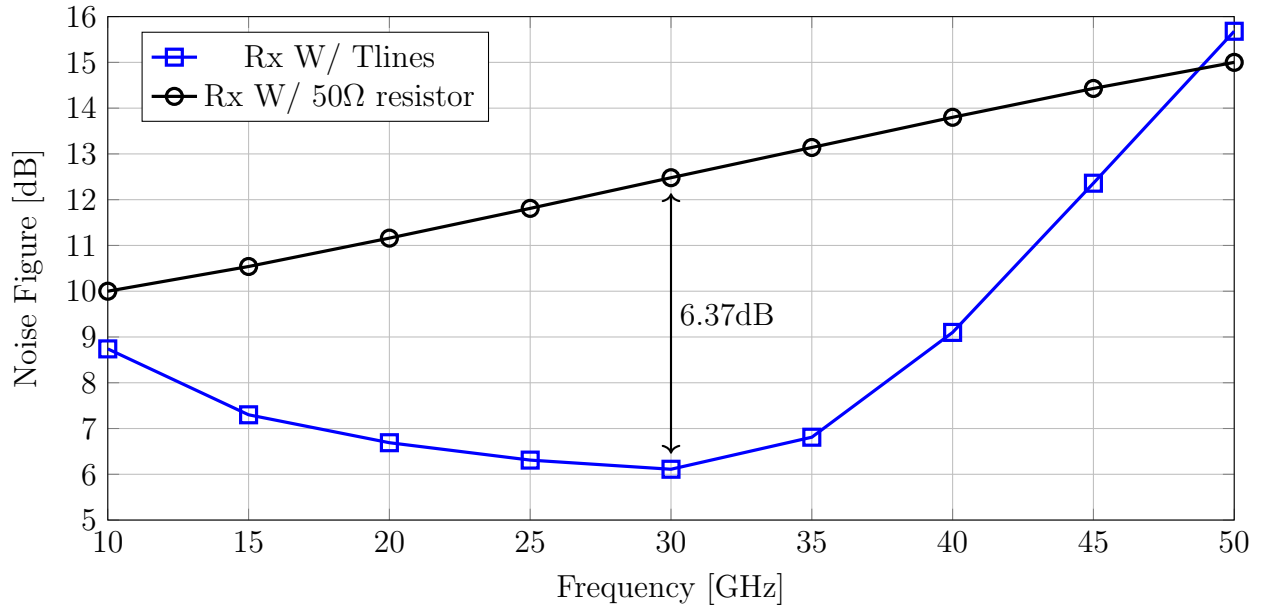


Figure 2.7: Noise figure of receiver with a  $50\Omega$  resistor and receiver with a  $\lambda/4$  transmission line designed for 30GHz

The simulation setup is similar to setup of the simulation with the full Wilkinson Divider. The only difference is that the bridge resistor is removed from the schematics. Figure 2.6 shows the simulation results of the design. There is a 4.7dB improvement in the noise figure compared to the  $50\Omega$  resistors design proposed in [7] at 20GHz. Figure 2.7 also shows the simulated noise figure values for the same design with transmission lines designed for 30GHz with a 6.37dB improvement in the noise figure. The higher frequency means a shorter length for the quarter-wavelength transmission lines, less loss in the signal path, and an improved noise figure.

## Limitations

Using transmission lines in mixer-first receivers provided a significant improvement in the noise figure. But the use of them is limited due to several factors. At 20GHz, the required length of a quarter-wavelength transmission line at is about 2mm. This means that the design will consume a large area and will not be practical. Additionally, this receiver design is still narrowband since matching will only be achieved at a single frequency. Chapter 3

provides a possible solution to this limitation.

## Chapter 3

# Mixer-first Receiver with Tunable Matching Network

This chapter discusses a new receiver design to overcome the area and the bandwidth limitation imposed by the designs proposed in the previous chapter. In this design, the quarter-wavelength transmission line is replaced with a passive L-matching network. The matching network will behave as an artificial quarter-wavelength transmission lines and it will transform the on-resistance of the mixers' to match the  $50\Omega$  resistance of the antenna. Figure 3.1 shows the receiver with the passive L-matching network. The matching network is used on both the I and the Q paths. It behaves as a low-pass filter to isolate the I and Q paths by filtering the charge sharing current between the two paths due to the overlapping LO waveform. It consists of a shunt cap at the input and a series inductor. This configuration is chosen as opposed to the capacitor in series and a shunt inductor because the series inductor would provide filtering to the charge sharing current, which is a technique proposed in [2]. The use of a L-matching network is an improvement from the previous design because a 2 mm transmission line is no longer needed, which puts less constraint on the area.

Fig. 3.2 shows the simulation results of the three receiver designs. The improvement in noise figure with the use of the passive matching network is similar to the improvement seen with the transmission lines design. The receiver design with the passive L-matching network is slightly better than the design with the transmission lines due to the use of lossless components in the matching network.

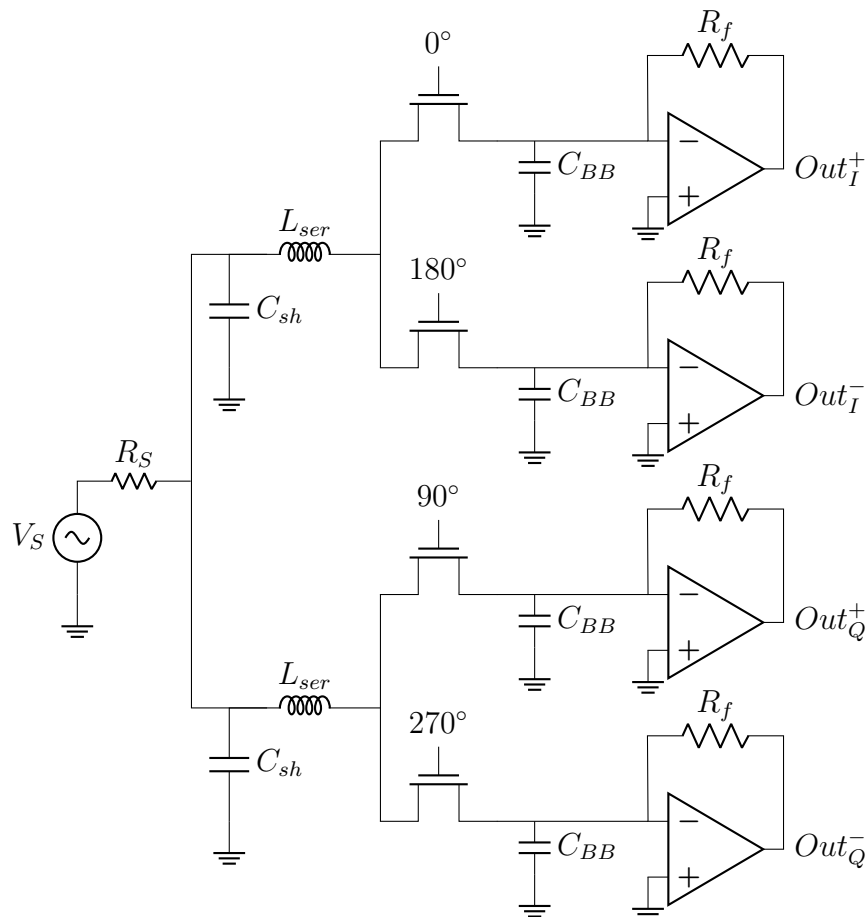


Figure 3.1: Mixer-first receiver with L-matching network

### Tunable Matching Network

Using passive components in the matching network will provide the possibility of using the receiver in wideband applications. To design a wideband receiver, the matching network needs to be tunable. This means that both the inductor and the capacitor should be adjustable. Figure 3.3 shows the schematic of the receiver with the tunable matching network. The variable capacitor can be implemented with either a varactor or a capacitor bank. The tunability of the inductor is more difficult to realize since inductors occupy larger amounts of area and implementing an inductor bank would be difficult. Hence, the variable inductor needs to be implemented using a different approach. In this design, the tunable inductor is implemented with an inductor in series with a capacitor bank. To see how this results

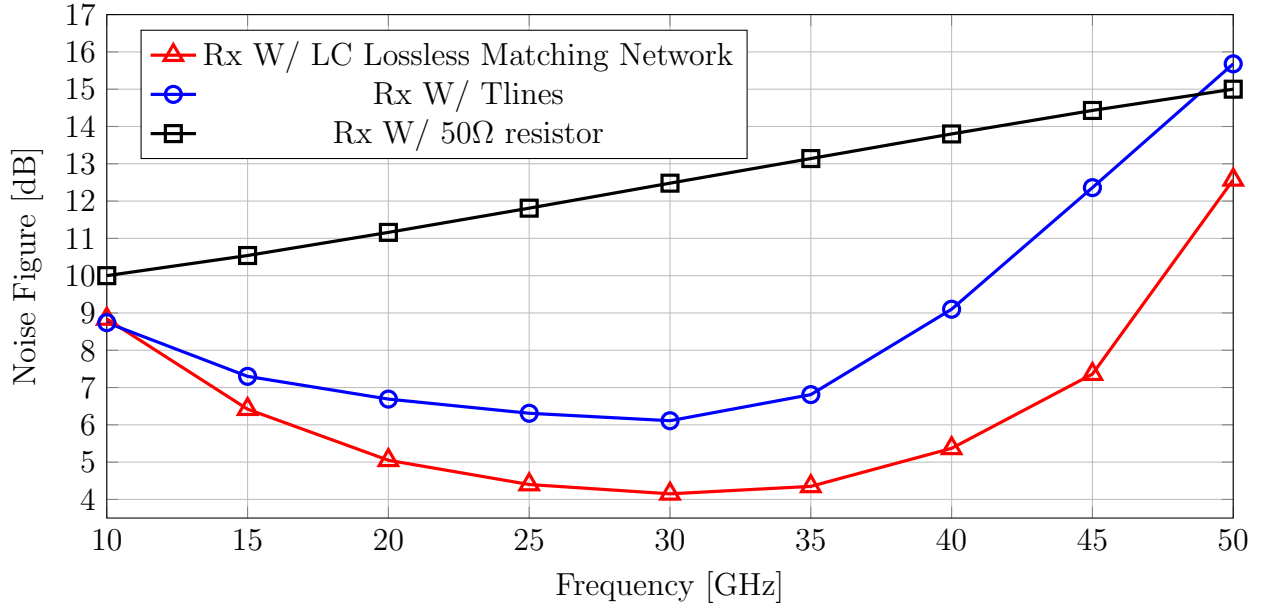


Figure 3.2: Comparison of NF across three different RX designs.

in a variable inductor, we can write the expression of the total impedance of the series combination. The series impedance of that combination can be written as

$$Z_{series} = j\omega L_{ser} + \frac{1}{j\omega C_{ser}} = j\left(\omega L_{ser} - \frac{1}{\omega C_{ser}}\right) \quad (3.1)$$

By looking at equation 3.1, it can be shown that changing the value of the series capacitor has the same effect as implementing a variable inductor. Decreasing the value of the series capacitor while keeping the inductor fixed will be the equivalent to decreasing the value of the inductor.

The shunt capacitor can be implemented with a varactor since its values vary slightly over different frequencies. The series capacitor needs to be implemented with a capacitor bank.

### 3.1 Linearity

The linearity of the receiver is governed by the linearity of the mixers and the baseband amplifier. This can be seen by analyzing the overall IIP3 of the receiver which is given with

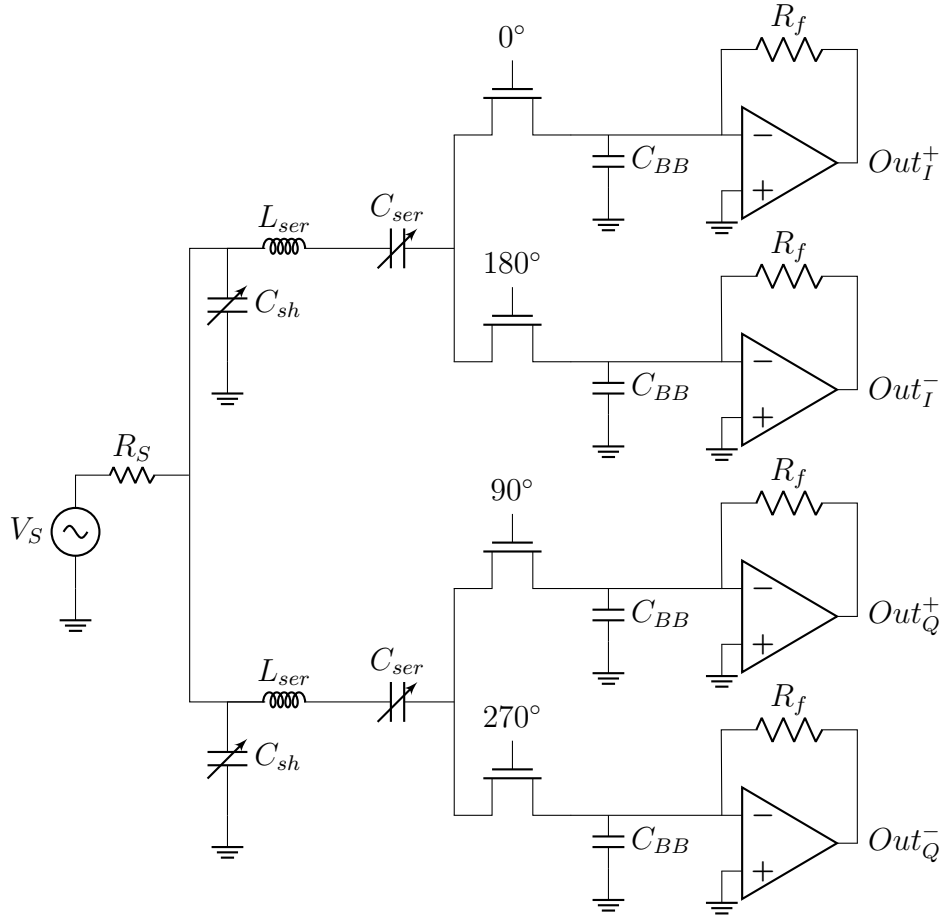


Figure 3.3: Mixer-first receiver with tunable L-matching network.

the following equation:

$$\frac{1}{V_{IIP3}^2} = \frac{a_{MN}^2}{V_{IIP3,mixer}^2} + \frac{a_{MN}^2 a_{mixers}^2}{V_{IIP3,BB}^2} \quad (3.2)$$

The gain of a 4-phase mixer,  $a_{mixers}$ , is approximately 1. Since the matching network steps down the voltage, the voltage gain of the matching network,  $a_{MN}$ , will be less than unity. This means that the technique of using matching networks effectively increases the IIP3 of the mixers. The linearity limit imposed by the baseband amplifier is mitigated by using feedback linearization, which is a technique previously proposed in [7]. By choosing a large open loop gain of the baseband amplifier, the input of the baseband amplifier can be nearly a virtual ground. This can be visualized in figure 3.4, where  $V_x$  would be almost zero by design. Making the input of the baseband amplifier's a virtual ground means that

input swing to the baseband amplifier is minimized which limits the effect of the baseband non-linearity on the receiver's overall linearity.

As for the mixers' linearity imposed by the the mixers'  $V_{gs}$  swing, the large gain of the baseband amplifier means that source terminal of the mixer, which is the input to the baseband amplifier, is a virtual ground. This will reduce the  $V_{gs}$  swing of the mixers. This concept is similar to the concept of "bottom-plate" mixers discussed in [9].

The linearity limit imposed by the the mixers'  $V_{ds}$  swing is mitigated by stepping down the input voltage with the matching network and using a smaller on-resistance for the mixers. Figure 3.4 shows a simplified schematic of the receiver and the effect of using the matching network on  $V_{ds}$  of the mixers. Assuming that the matching network is ideal, the output power of both matching networks will be

$$P_{out} = \frac{P_{in}}{2} \quad (3.3)$$

The power at the input,  $P_{in}$ , can be expressed as

$$P_{in} = \frac{V_{in}^2}{2R_s} \quad (3.4)$$

And the output power of the matching network can be expressed as

$$P_{out} = \frac{V_{ds}^2}{2R_{sw}} \quad (3.5)$$

Solving for  $V_{ds}$  in terms of  $V_{in}$  by plugging 3.5 and 3.4 into 3.3:

$$V_{ds} = \frac{v_s}{2} \sqrt{\frac{R_{sw}}{2R_s}} \quad (3.6)$$

With  $R_{sw} = 12\Omega$  and  $R_s = 50\Omega$ :

$$V_{ds} = \frac{v_s}{2} \sqrt{\frac{R_{sw}}{2R_s}} = \frac{v_s}{2} \sqrt{\frac{12}{100}} = 0.17V_s \quad (3.7)$$

Equation 3.7 shows that for smaller  $R_{sw}$ , the drain-source voltage swing will decrease improving the linearity of the receiver.

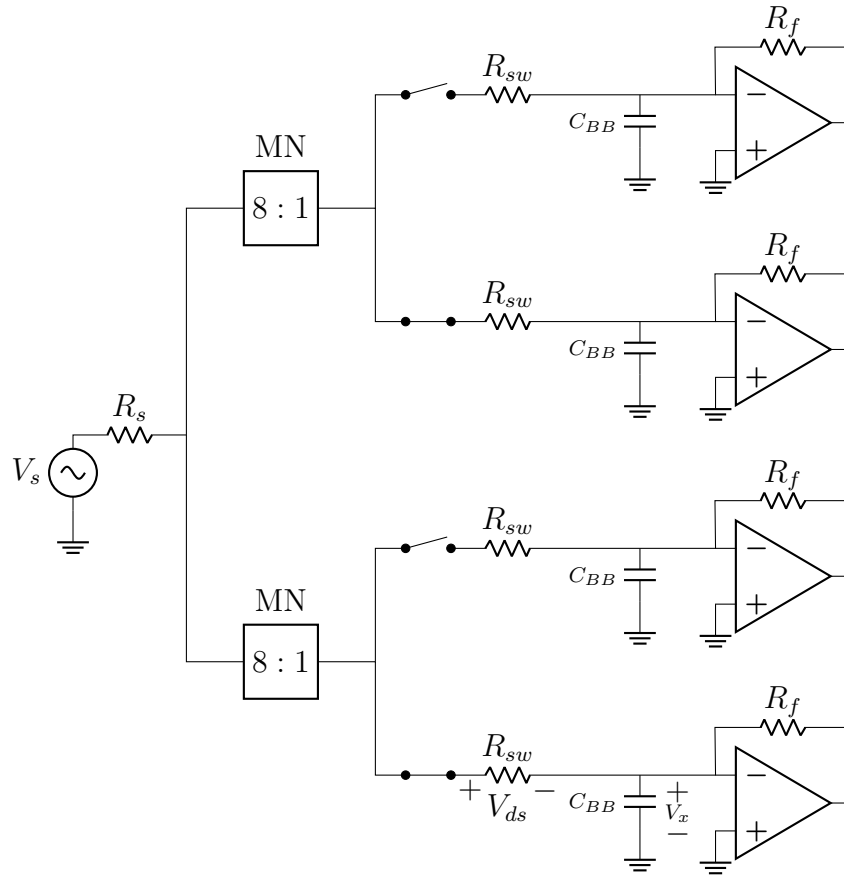


Figure 3.4: Simplified schematics of figure 3.3

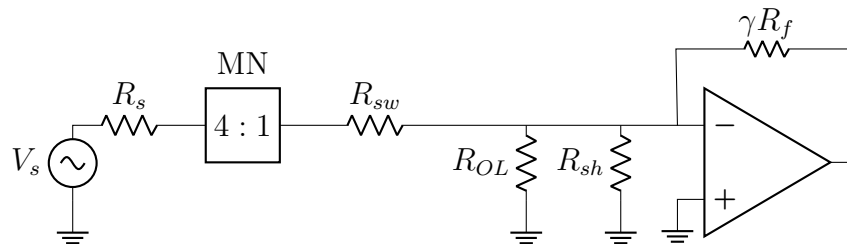


Figure 3.5: LTI equivalent circuits for figures 3.3 and 3.4.  $R_{sh}$  is the re-radiation resistance and  $R_{OL}$  is the overlap resistance. The two 8:1 matching networks in figure 3.4 can be replaced by one 4:1 matching network in the LTI model

## 3.2 Noise Figure

As discussed in chapter 1, the noise figure of the design proposed in [7] is high due to the use of a  $50\Omega$  resistor and the charge sharing current caused by the overlapping LO waveform. In addition to eliminating the physical resistor from the design, this design help improve the noise figure in other ways.

Figure 3.5 shows the linear time invariant model (LTI model) of the proposed design. The noise figure of the design can be expressed with the following equation:

$$F = 1 + \frac{R_{sw}}{R_s} + \frac{R_{sh}}{R_s} \left( \frac{R_{sw} + R_s}{R_{sh}} \right)^2 + \frac{R_{OL}}{R_s} \left( \frac{R_{sw} + R_s}{R_{OL}} \right)^2 \quad (3.8)$$

The noise of the baseband amplifier is neglected for simplicity and the matching network is assumed to be lossless and ideal. If the losses of the matching network are to be included, the loss can be modeled as a series resistor and it can be added to  $R_{sw}$  in equation 3.8.  $R_{OL}$  is the overlap resistor that is used to model the charge sharing effect and  $R_{sh}$  is the re-radiation resistor of the receiver.

## LO Harmonic Suppression

The proposed architecture in figure 3.3 offers LO harmonic filtering. The presence of high frequency LO harmonics means that interferes at those frequencies will be down converted to baseband, degrading the signal-to-noise ratio at the output and the receiver's noise figure. The matching network between the antenna and the mixer acts as a low-pass filter. Interferes at the LO harmonics will be attenuated before getting down converted to baseband. This will improve the signal-to-noise ratio at the output and will improve the noise figure as opposed to the design in [7]. The filtering effect makes this receiver architecture a harmonic rejection receiver. Unlike conventional harmonic rejection receivers, the tunable nature of the matching network allows for wideband operation.

In addition to being a harmonic rejection receiver, the matching network works as a filter for the current flowing from the mixers to the antenna. In equation 3.8, [3] showed that  $R_{sh}$  is due to the power losses resulting from the up-conversion of the LO harmonics to the antenna.  $R_{sh}$  can be expressed as the parallel combination of the antenna's impedance at

the odd harmonics of the LO. Since the matching network is a low pass filter, the impedance looking at the antenna from the mixers side would be large.

The large value of  $R_{sh}$  would translate to less loss in the receiver and that would improve the noise figure. Equation 3.8 shows how with increasing  $R_{sh}$ , the term where  $R_{sh}$  appears would tend to zero with increasing  $R_{sh}$ .

## Charge Sharing

In addition to being part of the matching network, the series inductor in the matching network offers another benefit, which is providing filtering to the charge sharing current the I and Q paths. This will consequently improve the noise figure of the receiver. The use of an inductor is also reported in [2] to reduce charge sharing.

To capture the effect of charge sharing, the resistor  $R_{OL}$  is used to model the effect of the overlapping LO waveform in the LTI model in figure 3.5 and the noise figure expression 3.8.  $R_{OL}$  is proportional to the resistance per path of the N-path filter and inversely proportional to the overlap time between the LO waveform.

$R_{OL}$  can be approximated using the following equation [6]:

$$R_{OL} \propto \frac{R_{path}}{\omega_{LO}\tau_{overlap}} \quad (3.9)$$

Where  $R_{path}$  is the resistance per path,  $\omega_{LO}$  is the angular frequency of the LO, and  $\tau_{overlap}$  is the overlapping time constant. With non-overlapping waveforms, the overlapping time is zero which makes  $R_{OL}$  is infinite.

## 3.3 Circuit Implementation

### Baseband Amplifier

The baseband amplifier is implemented with an inverter-based amplifier shown in figure 3.7. The size of the NMOS device is  $W/L=240\mu\text{m}/200\text{nm}$ , the size of the PMOS device  $W/L=300\mu\text{m}/200\text{nm}$ , and the current is 4.3mA. The feedback resistor is programmable.

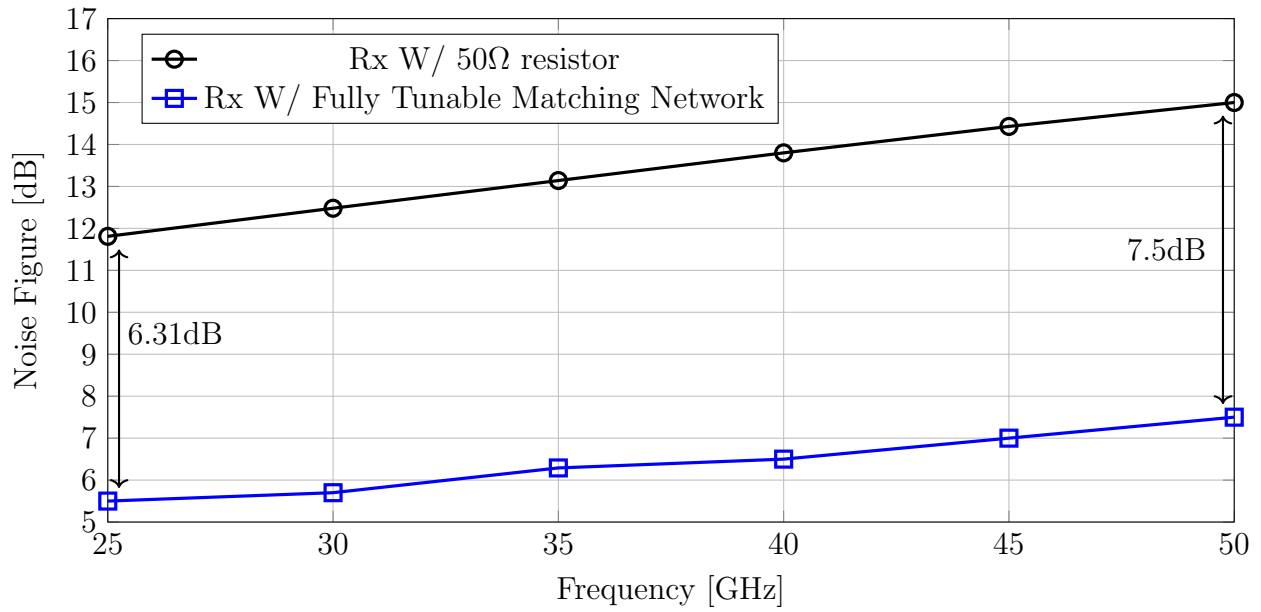


Figure 3.6: Noise figure values of the proposed linear receiver compared to the design proposed in the previous chapter. Ideal LO, baseband amplifier, and  $R_{sw} = 6\Omega$

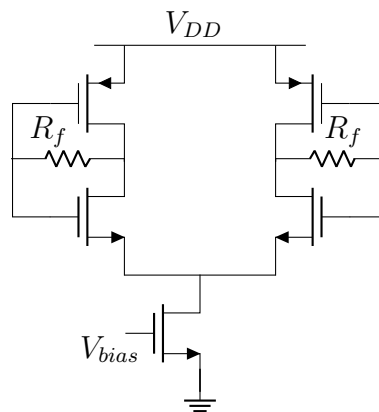


Figure 3.7: Inverter-based baseband amplifier

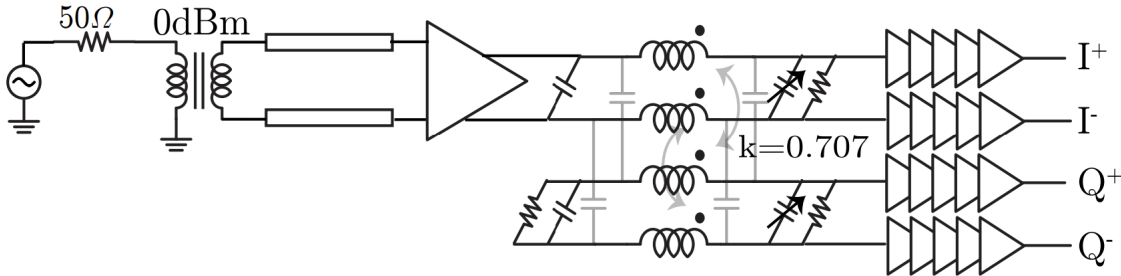


Figure 3.8: Schematic of the LO Chain [6].

## LO Chain

The LO chain used is shown in figure 3.8. The single-ended LO input is converted to a differential waveform using a balun. Using inverter-based buffers, the differential waveform is fed into a quadrature hybrid to generate the four-phase 50% LO waveforms. Inverter-based LO buffers are also used after the quadrature hybrid to drive the mixers. This LO chain used is similar to the one used in [7].

## Mixers' Sizes

The choice of the mixers' size affects the performance of the receiver. Choosing a large device would make the on-resistance of the mixer smaller, improving the noise figure. The simulation results showed a 0.3dB improvement in the noise figure when using a switch with on-resistance  $6\Omega$  instead of  $12\Omega$ . The mixers' are driven by an ideal voltage source with overlapping LO waveforms.

The larger transistor size, however, means that the gate capacitance of the mixers will be larger, making it more difficult to drive the mixers with a reasonable power consumption through the LO chain. Figure 3.9 shows the simulations results of the receiver with mixers with  $W/L = 27\mu\text{m}/30\text{nm}$  ( $R_{sw} = 12\Omega$ ) vs  $W/L = 54\mu\text{m}/30\text{nm}$  ( $R_{sw} = 6\Omega$ ). The larger mixers also mean adding more parasitic capacitance to the input of the mixer, leading to more loss in the signal path and further degradation in the noise figure. Hence, the final design uses switches with  $W/L = 27\mu\text{m}/30\text{nm}$  instead of a larger device size, with  $R_{sw} = 12\Omega$ .

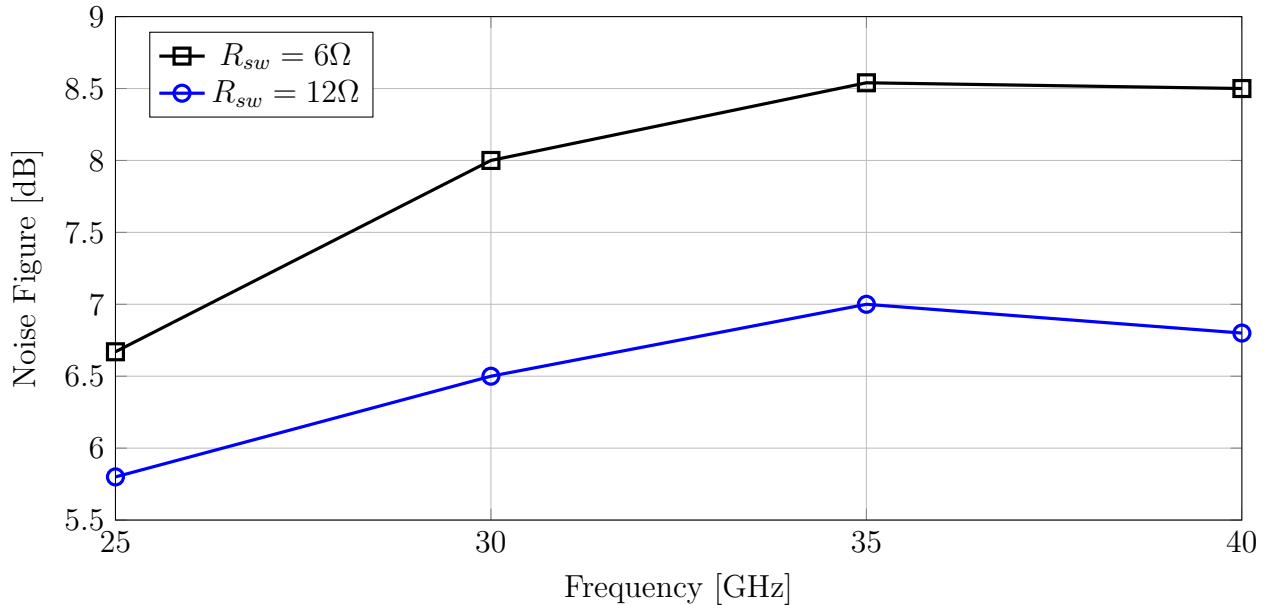


Figure 3.9: Noise figure of Rx with fully tunable lossy L-matching networks, transistor switches, and LO chain

## Matching Network Implementation

The pad and the ESD capacitance at the input can be included in the implementation of the shunt capacitor. The inductors are implemented with octagonal single-turn configuration to maximize the quality factor. The inductors have a self-resonance frequency of 110GHz and the quality factor achieved varies from 9.5 - 11.8 across the frequency range of 25GHz-40GHz. Figure 3.10 shows the layout of the inductors. The currents in the inner most branch are in the same direction, which means that mutual inductance will increase the total inductance of both inductors. The series capacitor is implemented with a capacitor bank.

Figure 3.12 shows the final results of the post-layout simulated design.  $R_f = 1\text{ k}\Omega$  is used. The well known discontinuities in the BSIM4 [15] models made it difficult to simulate IP3 of the receiver. The source of the discontinuities are transistors in deep triode region, which in this case are the mixers. The mixers were replaced by ideal switches to simulate the IP3.

Figure 3.13 shows Noise summary results in virtuoso. The figure shows that the noise of the and the inductor feedback resistor,  $R_f$ , and the inductor are the main contributor's to

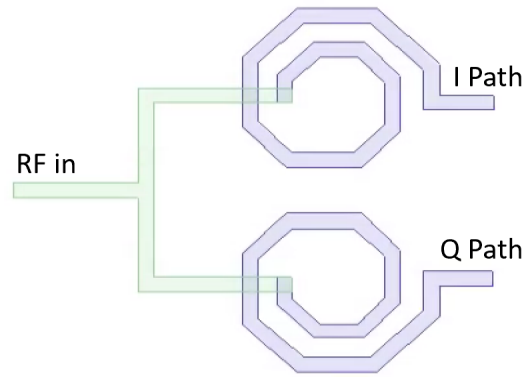


Figure 3.10: Inductors' Layout

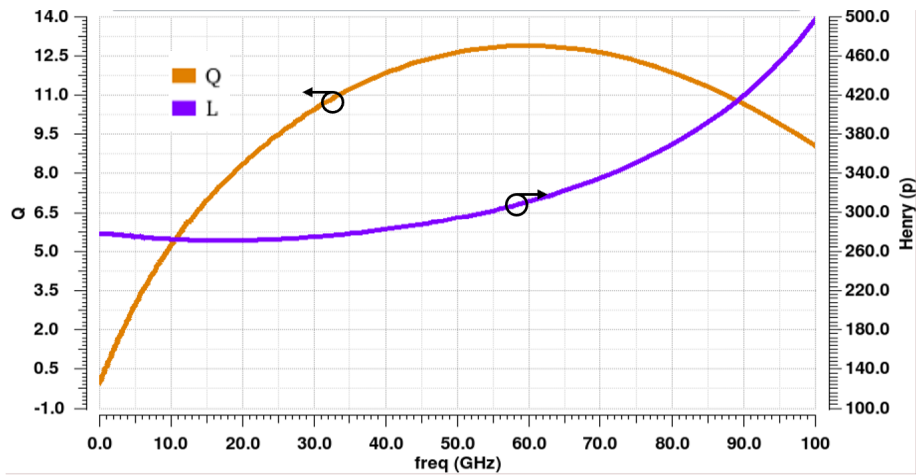


Figure 3.11: Inductors Q and L

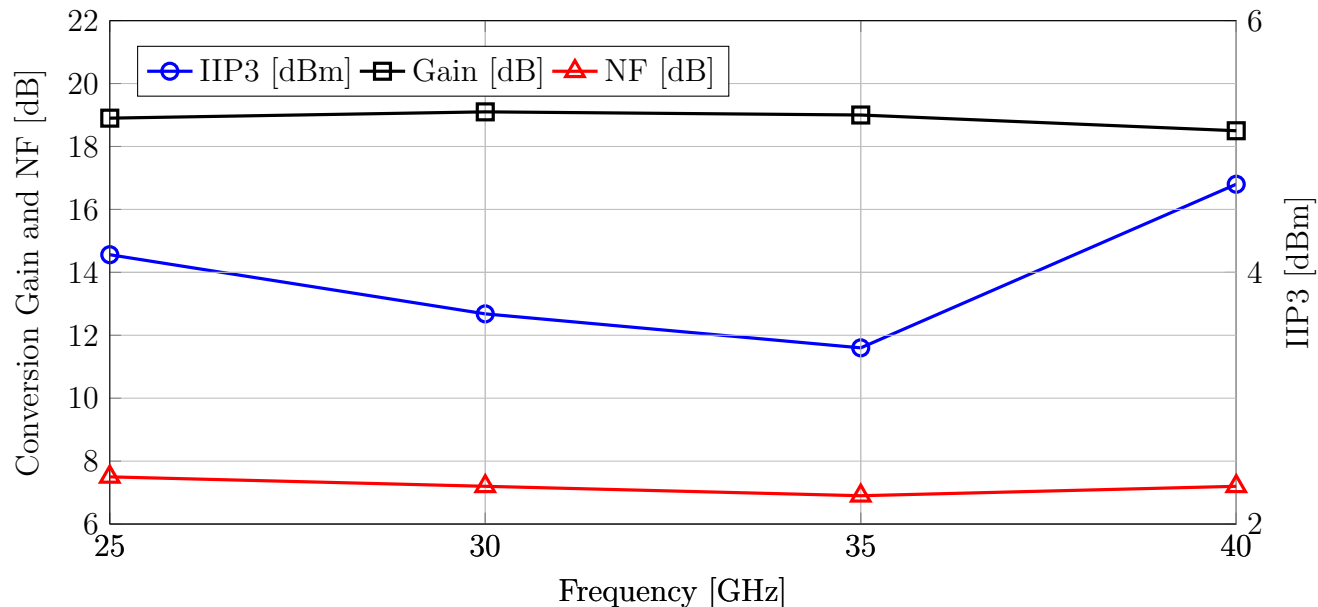


Figure 3.12: Post-layout Simulations of the design

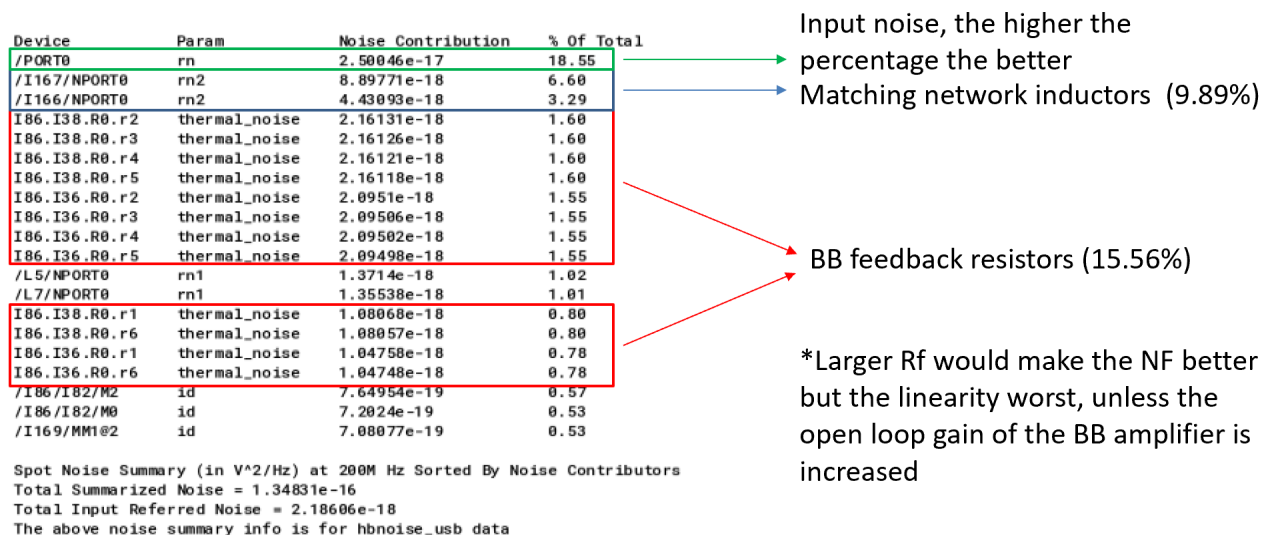


Figure 3.13: Noise summary results

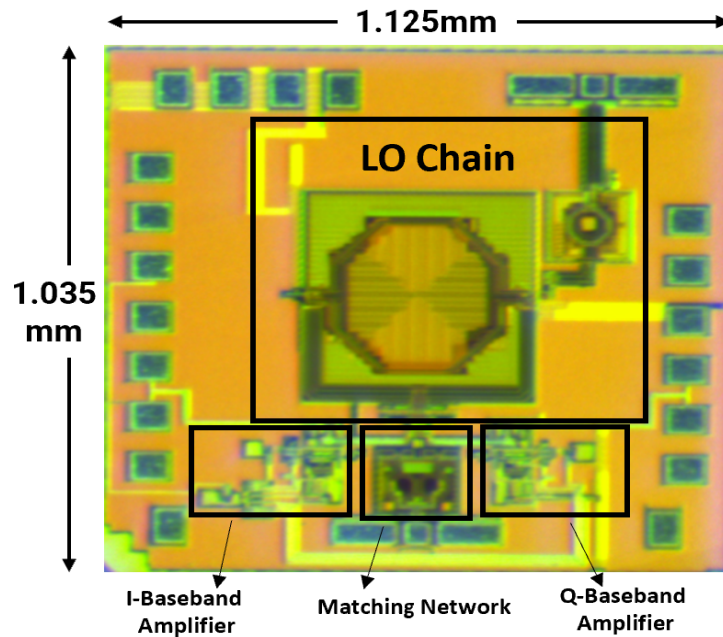


Figure 3.14: Chip micrograph in 28 nm bulk CMOS process

the overall receiver noise. Improving the quality factor of the inductor is a possible way of improving the performance of the receiver. Additionally, choosing a larger feedback resistor value will improve the noise figure but will increase the degrade the linearity of the receiver.

### 3.4 Measurements

The design was taped out in 28 nm bulk CMOS process and is awaiting measurement. Fig. 3.14 show a micrograph of the test chip. The chip is to be wirebonded to the PCB and the LO and the RF input are to be probed with GSG probes.

## Chapter 4

# Conclusion and Future Work

This thesis proposed multiple designs for linear mixer-first receivers. Chapter 2 explored a narrowband mixer-first receiver using a Wilkinson divider and a modified version of the Wilkinson divider. Chapter 3 explored a wideband mixer-first receiver using a tunable matching network. Post-layout simulations showed an improvement in noise figure values compared to the design proposed in [7]. The final design achieved a noise figure of less than 8dB from a frequency range of 25GHz to 40GHz, and an IIP3 of +3.6dBm to +4.2dBm across the frequency range. Table 4.1 shows a comparison between the proposed design and the state-of-the-art mixer-first receiver greater than 25GHz. The noise figure value are lower than the other reported noise figure values. Although the IIP3 numbers are lower compared to the values reported in [7], the values are improved compared to the other designs listed. The in-band IP3 values of the receiver can be improved by using a baseband amplifier with a large open loop gain. The larger amplifier gain would further minimize the swing at the input of the baseband amplifier, which will consequently improve the linearity of the receiver. Improving the LO Chain will deliver a better LO waveform to the mixers which would help with the linearity of the switch and the overall performance of the receiver.

Table 4.1: Comparison with mixer-first receivers greater than 25GHz

	<b>Moroni</b> [11] RFIC 2012	<b>Wilson</b> [13] RFIC 2016	<b>Krishna-</b> <b>murthy</b> [8] RFIC2019	<b>Iotti</b> [4] JSSC2020	<b>Ahmed</b> [1] CICC2020	<b>This</b> <b>work</b>
Technology	65nm CMOS	45nm SOI	28nm CMOS	28nm CMOS	22nm FD-SOI	<b>28nm</b> <b>CMOS</b>
$f_{RF}$ (GHz)	49 – 67	20–30	10 – 35	70 – 100	43 – 97	<b>25 – 40</b>
Voltage gain (dB)	13	8 – 20.6	11.5 – 14.5	19.5 – 25.3	12 – 15	<b>18</b> †
In-band IIP3 (dBm)	-	-2.3 – -9.7	+10 – +14.1	-	0 – +4	<b>+3.6 –</b> <b>+4.2</b> †
NF (dB)	11–14	8	12.5 – 19.2	8 – 12.7	12.5 – 16.5	<b>6.8 –</b> <b>7.5</b> ‡
DC power (mW)	14	41 (at 24GHz)	22.8 (Base- band); 19 – 37 (LO)	12	36	<b>22.8</b> (Base- band); <b>19 – 37</b> (LO)
Supply (V)	1.2	0.9/1.8	1.2	1	-	<b>1.2</b>

† Measurements reported at nominal setting ( $R_F = 1k\Omega$ ), across  $f_{LO}$ .

‡ NF varies from 6.8 – 7.5 dB for  $f_{LO} = 25 – 40GHz$ .

Table 4.2: Comparison with recently published 28GHz receiver front-ends

	<b>Yeh</b> [14] RFIC 2016	<b>Kibaroglu</b> [5] RFIC 2017	<b>Mondal</b> [10] JSSC2019	<b>Sadhu</b> [12] JSSC2017	<b>This work</b>
Technology	120nm SiGe	180nm SiGe	65nm CMOS	130nm SiGe	<b>28nm CMOS</b>
$f_{RF}$ (GHz)	28-32	28-32	28/37	28	<b>25 – 40</b>
Voltage gain (dB)	9.4	20	33/26.5	34	<b>18</b>
NF (dB)	5.1	4.6	7.3	6	<b>6.8 – 7.5<sup>#</sup></b>
DC power (mW)	136.5	130	52.5	103.1	<b>22.8</b> (Baseband); <b>19 – 37</b> (LO)

<sup>#</sup> NF varies from 6.8 – 7.5 dB for  $f_{LO} = 25 – 40$ GHz.

# Bibliography

- [1] A. Ahmed, M. Huang, and H. Wang. “Mixer-First Extremely Wideband 43 — 97 GHz RX Frontend with Broadband Quadrature Input Matching and Current Mode Transformer-Based Image Rejection for Massive MIMO Applications”. In: *2020 IEEE Custom Integrated Circuits Conference (CICC)*. 2020.
- [2] Caroline Andrews, Changhyuk Lee, and Alyosha Molnar. “Effects of LO harmonics and overlap shunting on N-phase passive mixer based receivers”. In: *2012 Proceedings of the ESSCIRC (ESSCIRC)*. 2012, pp. 117–120.
- [3] Caroline Andrews and Alyosha C. Molnar. “Implications of Passive Mixer Transparency for Impedance Matching and Noise Figure in Passive Mixer-First Receivers”. In: *IEEE Transactions on Circuits and Systems I: Regular Papers* 57.12 (2010), pp. 3092–3103.
- [4] Lorenzo Iotti et al. “A Low-Power 70-100-GHz Mixer-First RX Leveraging Frequency-Translational Feedback”. In: *IEEE Journal of Solid-State Circuits* 55.8 (2020), pp. 2043–2054.
- [5] Kerim Kibaroglu, Mustafa Sayginer, and Gabriel M Rebeiz. “An ultra low-cost 32-element 28 GHz phased-array transceiver with 41 dBm EIRP and 1.0–1.6 Gbps 16-QAM link at 300 meters”. In: *2017 IEEE Radio Frequency Integrated Circuits Symposium (RFIC)*. 2017, pp. 73–76.
- [6] Sashank Krishnamurthy. “Interference-Resilient CMOS Receiver Front-Ends for Next Generation Radios”. PhD thesis. EECS Department, University of California, Berkeley, Dec. 2021. URL: <http://www2.eecs.berkeley.edu/Pubs/TechRpts/2021/EECS-2021-231.html>.

- [7] Sashank Krishnamurthy, Lorenzo Iotti, and Ali M. Niknejad. “Design of High-Linearity Mixer-First Receivers for mm-Wave Digital MIMO Arrays”. In: *IEEE Journal of Solid-State Circuits* 56.11 (2021), pp. 3375–3387.
- [8] Sashank Krishnamurthy and Ali M Niknejad. “Enhanced Passive Mixer-first Receiver Driving an Impedance with 40dB/decade Roll-off, Achieving +12dBm Blocker-P1dB, +33dBm IIP3 and sub-2dB NF Degradation for a 0dBm Blocker”. In: *2019 IEEE Radio Frequency Integrated Circuits Symposium (RFIC)*. June 2019, pp. 139–142.
- [9] Yuan-Ching Lien et al. “High-Linearity Bottom-Plate Mixing Technique With Switch Sharing for  $N$ -path Filters/Mixers”. In: *IEEE Journal of Solid-State Circuits* 54.2 (2019), pp. 323–335.
- [10] Susnata Mondal and Jeyanandh Paramesh. “A reconfigurable 28-/37-GHz MMSE-adaptive hybrid-beamforming receiver for carrier aggregation and multi-standard MIMO communication”. In: *IEEE Journal of Solid-State Circuits* 54.5 (2019), pp. 1391–1406.
- [11] Anna Moroni and Danilo Manstretta. “A broadband millimeter-wave passive CMOS down-converter”. In: *2012 IEEE Radio Frequency Integrated Circuits Symposium*. 2012, pp. 507–510.
- [12] Bodhisatwa Sadhu et al. “A 28-GHz 32-element TRX phased-array IC with concurrent dual-polarized operation and orthogonal phase and gain control for 5G communications”. In: *IEEE Journal of Solid-State Circuits* 52.12 (2017), pp. 3373–3391.
- [13] Charley Wilson and Brian Floyd. “20–30 GHz mixer-first receiver in 45-nm SOI CMOS”. In: *2016 IEEE Radio Frequency Integrated Circuits Symposium (RFIC)*. 2016, pp. 344–347.
- [14] Yi-Shin Yeh et al. “A 28-GHz 4-channel dual-vector receiver phased array in SiGe BiCMOS technology”. In: *2016 IEEE Radio Frequency Integrated Circuits Symposium (RFIC)*. 2016, pp. 352–355.
- [15] Hazal Yüksel, Dong Yang, and Alyosha C. Molnar. “A circuit-level model for accurately modeling 3rd order nonlinearity in CMOS passive mixers”. In: *2014 IEEE Radio Frequency Integrated Circuits Symposium*. 2014, pp. 127–130.

# Appendix A

## Isolation in Wilkinson Dividers

In a Wilkinson's divider, the bridge resistor's main function is to isolate  $Port_2$  and  $Port_3$ . To calculate the resistor value required for isolation, we can find an expression for  $S_{23}$ , set it equal to zero and calculate the value of  $R_{br}$ .  $S_{23}$  can be calculated by applying a signal at  $Port_2$  and using differential and common mode circuit equivalent to calculate the total current flowing through the load resistor at  $Port_3$ . Figure A.1 shows differential and common mode circuit schematic. Figure A.1.b shows the common mode circuit equivalent where the line of symmetry is open and no current will flow through the bridge resistor. Figure A.1.c shows the common mode half circuit where the bridge resistor is omitted since no current is flowing through it. The common mode current flowing out of  $Port_3$  is equal to

$$i_{cm} = \frac{v_s/2}{R_L + Z_{TL}} \quad (\text{A.1})$$

Where  $Z_{TL}$  is the impedance looking into the transmission line from  $Port_3$ . And since it's a  $\lambda/4$  transmission line,  $Z_{TL}$  can be expressed as

$$Z_{TL} = \frac{Z_0^2}{2R_s} = R_L \quad (\text{A.2})$$

By plugging equation A.2 into equation A.1,  $i_{cm}$  can be expressed as

$$i_{cm} = \frac{v_s/2}{R_L + R_L} = \frac{v_s}{4R_L} \quad (\text{A.3})$$

Figure A.1.d shows the differential circuit half circuit. The source resistor,  $R_s$ , is omitted since it's grounded on both sides. The current through the transmission line,  $i_{tl}$  is zero

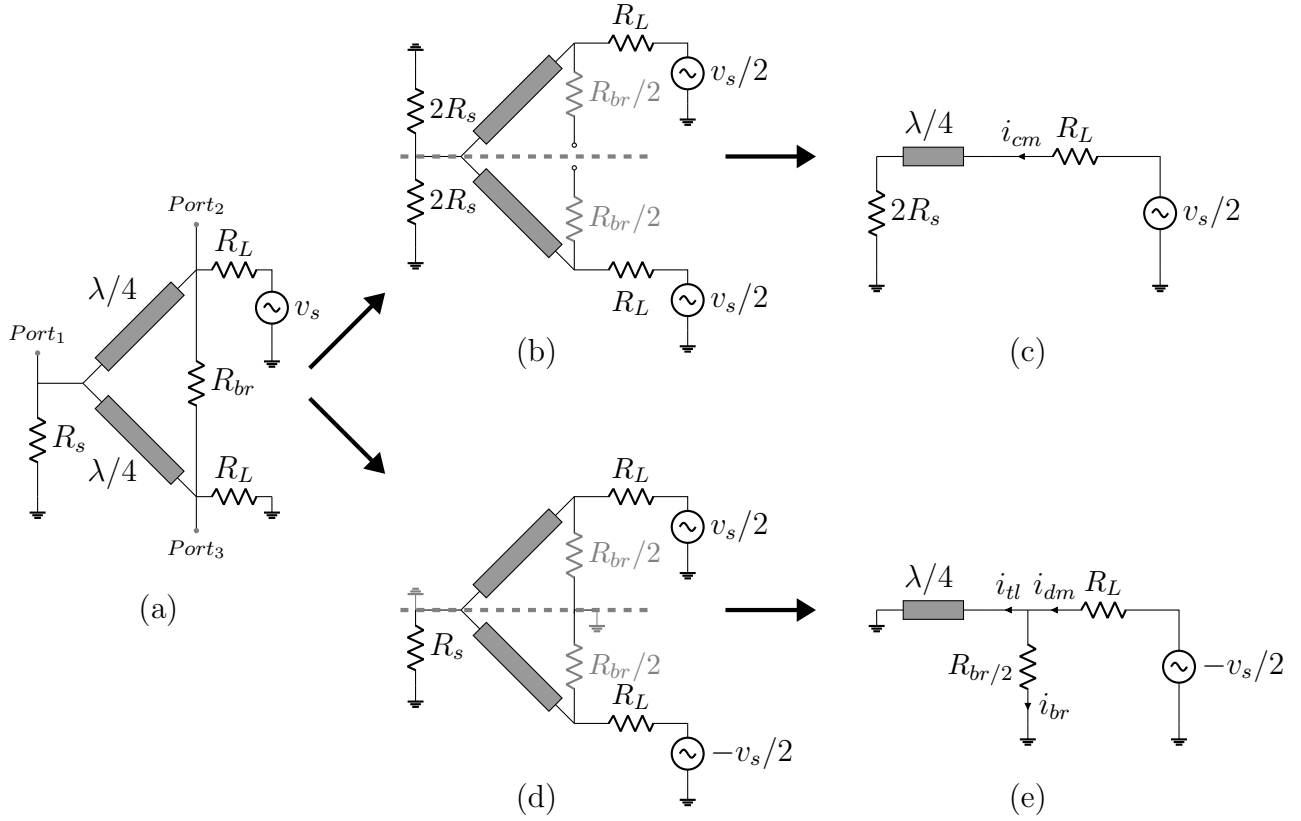


Figure A.1: Differential and common mode schematics. (a) Wilkinson divider. (b) Wilkinson divider in common mode. (c) Wilkinson divider common mode half circuit. (d) Wilkinson divider in differential mode. (e) Wilkinson divider differential mode half circuit.

because the impedance looking into it is infinite since it's a shorted  $\lambda/4$  transmission line.

This makes

$$i_{dm} = i_r = \frac{-v_s/2}{R_L + R_{br}/2} = \frac{-v_s}{2R_L + R_{br}} \quad (\text{A.4})$$

By superposition, the total current through  $Port_3$  is

$$i_{P3} = i_{dm} + i_{cm} \quad (\text{A.5})$$

By substituting A.4 and A.3 in A.5,  $i_{p3}$  can be expressed as:

$$i_{P3} = \frac{-v_s}{2R_L + R_{br}} + \frac{v_s}{4R_L} \quad (\text{A.6})$$

For the  $Port_2$  and  $Port_3$  to be isolated, the current through  $Port_3, i_{p3}$ , needs to be zero.

By setting the current,  $i_{p3}$ , to zero and solving for  $R_{br}$ ,

$$i_{P3} = \frac{-v_s}{2R_L + R_{br}} + \frac{v_s}{4R_L} = 0 \quad (\text{A.7})$$

we obtain the value of the Bridge resistor. This makes the required value for  $R_{br} = 2R_L$